Role of Glutamate 91 in Information Transfer during Substrate Activation of Yeast Pyruvate Decarboxylase†

Haijuan Li,‡ William Furey,§ and Frank Jordan*,‡

Departments of Chemistry and Biological Sciences and Program in Cellular and Molecular Biodynamics, Rutgers, the State University, Newark, New Jersey 07102, and Department of Biocrystallography, VA Hospital, P.O. Box 12055, University Drive, Pittsburgh, Pennsylvania 15240

Received February 2, 1999; Revised Manuscript Received May 19, 1999

ABSTRACT: Oligonucleotide-directed site-specific mutagenesis was carried out on pyruvate decarboxylase (EC 4.1.1.1) from *Saccharomyces cerevisiae* at E91, located on the putative substrate activation pathway and linking the α and γ domains of the enzyme. While C221 on the β domain is the residue at which substrate activation is triggered [Baburina, I., et al. (1994) *Biochemistry 33*, 5630−5635; Baburina, I., et al. (1996) *Biochemistry 35*, 10249−10255], that information, via the substrate bound at C221, is transmitted to H92 on the α domain, across the domain divide from C221 [Baburina, I., et al. (1998) *Biochemistry 37*, 1235−1244], thence to E91 on the α domain, and then on to W412 on the γ domain [Li, H., and Jordan, F. (1999) *Biochemistry 38*, 10004−10012] and to the active site thiamin diphosphate located at the interface of the α and γ domains [Arjunan, D., et al. (1996) *J. Mol. Biol. 256*, 590−600]. Substitution at E91 with Q, D, or A led to modest reductions in the specific activity (4-, 5-, and 30-fold), as well as in both the turnover number and the catalytic efficiency, in that order. Interestingly, the Hill coefficient was only slightly reduced for the E91D variant, but cooperativity was virtually abolished for the E91Q and E91A variants. The thermal stability of the variants was reduced in the following order: wild type > E91Q > E91D > E91A; circular dichroism and fluorescence experiments also demonstrated that the tertiary structure of the enzyme was affected by these substitutions. The variants could be purified as apoenzymes, demonstrating their impaired ability to bind thiamin diphosphate. Apparently, the charge at residue 91 is quite important for maintaining optimal cooperativity. To maintain strong domain−domain interactions, the length of the side chain at position 91 with hydrogen bonding potential to W412 is sufficient.

Yeast pyruvate decarboxylase (PDC,[1] EC 4.1.1.1) is one of several enzymes that participate in nonoxidative functions of thiamin diphosphate (ThDP, the vitamin B_1 coenzyme). PDC converts pyruvate to acetaldehyde and carbon dioxide (see Scheme 1; for reviews, see refs *1*−*7*). The enzyme also has a requirement for a divalent cation, best fulfilled by Mg(II), and its presence as part of the diphosphate binding locus had been earlier confirmed by structural studies of ThDP-dependent enzymes (*8*).

PDC from yeast is subject to substrate activation (*9*, *10*), and it was proposed that a cysteine side chain may be responsible for this activation (*11*, *12*). PDC from *Saccharomyces cerevisiae* (scpdc1; *13*) is comprised of 563 amino acids, and each subunit possesses four cysteines at positions 69, 152, 221, and 222, none of which participate in disulfide bridges. The three-dimensional structures of PDC from *Saccharomyces uvarum* (supdc1; *14*) and scpdc1 (*15*) have revealed that C221, the cysteine nearest to ThDP, is >20 Å away from the reaction center, the C2 atom of the thiazolium ring on ThDP. The ThDP resides in a cleft between the α and γ domains on different subunits. The Cys side chains at positions 221 and 222, most favorably positioned for a potential regulatory function, reside on the β domain (*14*, *15*). In earlier studies from these laboratories, it was first shown that a pdc1−6 fusion enzyme (consisting of amino acids 1−45 derived from the *PDC1* gene and 46−563 derived from the *PDC6* gene) with its single cysteine at position 221 can still be activated by pyruvate (*16*). Next, the C221S and C222S (single-site) and C221S/C222S (two-site) mutant yeasts were constructed, and then the genes were transferred into a high-expression level *Escherichia coli* vector for further mutagenesis studies. It was convincingly shown that substitution of C221, but not of C222, with serine (*17*) or alanine (*18*) leads to the abolition of substrate activation, thereby identifying C221 as the site at which substrate, or the substrate surrogate pyruvamide (that can also activate the enzyme but cannot be decarboxylated; see ref *10*), is bound, via either a covalent or a noncovalent linkage. A third cysteine, C152, while accessible, is not

† Supported at Rutgers by NIH Grant GM-50380, NSF Training Grant BIR 94/13198 in Cellular and Molecular Biodynamics (F.J., principal investigator), the Rutgers University Busch Biomedical Fund, Hoffmann La Roche Diagnostics Inc. (Somerville, NJ) and in Pittsburgh by NIH Grant GM-48195 (to W.F.).

* To whom correspondence should be addressed. Telephone: (973) 353-5470. Fax: (973) 353-1264. E-mail: frjordan@newark.rutgers.edu.

‡ Rutgers, the State University.

§ VA Hospital.

[1] Abbreviations: ThDP, thiamin diphosphate; PDC, pyruvate decarboxylase (EC 4.1.1.1); scpdc1, wild-type pyruvate decarboxylase isolated from *Saccharomyces cerevisiae* and overexpressed in *Escherichia coli*; WT, wild-type PDC; E91A, E91D, and E91Q, variants of PDC; SDS−PAGE, sodium dodecyl sulfate−polyacrylamide gel electrophoresis; PMSF, phenylmethanesulfonyl fluoride; n_H, Hill coefficient.

10.1021/bi9902438 CCC: $18.00
Published on Web 07/16/1999

Scheme 1

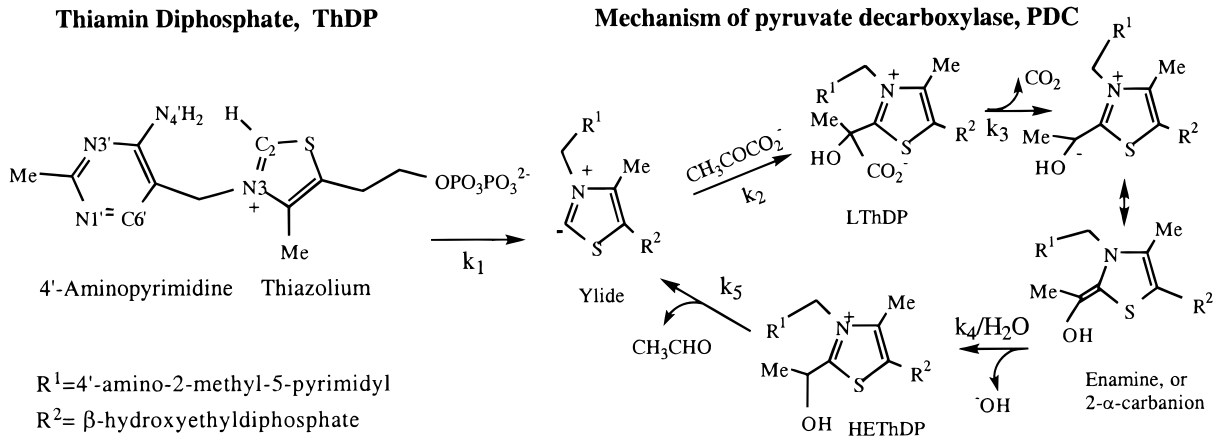

favorably positioned to interact with substrate. FT-IR and isoelectric focusing experiments were carried out with several variants of scpdc1, providing evidence that of the four cysteines, only C152 is undissociated near pH 6 (*19*). Protein chemical evidence also points to the unique high reactivity of C221 (*20*).

According to isoelectric focusing experiments, residue H92 is probably protonated at pH 6.0, the pH optimum of the enzyme. Molecular modeling (*15*) suggested that pyruvate bound to C221 could reach over to, and interact with, H92. Directed mutagenesis carried out at H92 on the α domain, across the domain divide from C221, showed that substitution at H92 with G, A, or C leads to great reduction of the Hill coefficient (from 2.0 in the wild-type enzyme to 1.2−1.3), while substitution for Lys affords an active enzyme with a Hill coefficient of 1.5−1.6. 1,3-Dibromoacetone, a potential cross-linker when added to the H92C/C222S variant at a concentration of 0.1 mM, abolished substrate activation while reducing the activity only by 30%. Therefore, 1,3-dibromoacetone may cross-link C92 and C221. It was concluded that H92 is on the information transfer pathway during the substrate activation process and the interaction between C221 on the β domain and H92 on the α domain is required for substrate activation. Extensive pH studies of the steady-state kinetic constants provided support for the interaction of C221 and H92 and the transmission of regulatory information to the active center via this pathway and pK_a values for the two groups, approximately 5.2 for C221 and 6.4 for H92 (*18*, *20*).

The molecular modeling study (*15*) also suggested that if C221 forms a hemithioketal with the α-keto group of pyruvate, unfavorably short contacts are formed with H92 of the α domain, which should make either the C221, H92, or both move to accommodate the adduct. Perturbation of the side chain of H92 would displace the adjacent E91 somewhat. The side chain of E91 makes numerous van der Waals contacts with a short segment containing residues 410−415 of the γ domain, as well as a hydrogen bond to the main chain NH of W412, the latter of which in turn can transmit subtle distortions to the adjacent G413, whose main chain carbonyl oxygen provides one of the conserved hydrogen bonds to the 4′-aminopyrimidine of ThDP at the active site. Our current working hypothesis is that the consequences of binding substrate at C221 are propagated to the active site via the pathway H92 → E91 → W412 → G413 → ThDP.

To investigate the function of E91 on the α domain in the substrate activation process, E91 was substituted with D, Q, or A via site-directed mutagenesis. In the accompanying paper, we complete exploration of this putative substrate activation pathway by also examining effects of substitution on kinetics, thermostability, and tertiary structure at residue W412.

EXPERIMENTAL PROCEDURES

Materials. *Nde*I and *Sca*I restriction enzymes and the corresponding buffers were purchased from Promega. *Pfu* DNA polymerase and T4 DNA ligase were purchased from Stratagene. Coomassie Plus Protein Assay Reagent was purchased from Pierce. Centriprep-30 and Centricon-30 devices were purchased from Amicon. Superdex 200 and DEAE-FF were purchased from Amersham Pharmacia Biotech. Bis-Tris and Amberlite MB-150 were purchased from Sigma.

Construction of the E91A PDC Variant. Site-directed mutagenesis of the *PDC1* gene to convert E91 to A was carried out according to the instructions of the Chameleon Double-Stranded Site-Directed Mutagenesis Kit from Stratagene (*21*). The pET22b(+) vector containing the *PDC1* gene was heat denatured and annealed with two oligonucleotide primers. One primer (selection primer), 5′-CTGTGACTG-GTG*ACGCGT*CAACCAAGTC-3′, changed the unique *Sca*I restriction site on the Amp gene to a *Mlu*I restriction site, by changing the nucleotide sequence from AGTACT to ACGCGT (italics). Another primer, 5′-GCCGGTTCATAT-GCT**GCC**CACGTCGGTG-3′ (the mutagenic primer), changed the glutamic acid at position 91 to alanine by mutating codon 91 from GAA to GCC (bold), and created a *Nde*I restriction site for mutant screening, via silent mutations from TCTTAC to TCATAT (underlined). The plasmid was denatured, and primers were annealed to the plasmid. The plasmid DNA was digested with the *Sca*I restriction enzyme; the resultant DNA digest was transformed into *E. coli* XL1-Blue competent cells, and the cells were grown overnight at 37 °C on the LB−ampicillin agar plates (10 g of NaCl, 10 g of tryptone, 5 g of yeast extract, 20 g of agar, and 100 mg of ampicillin per liter).

The colonies were screened for the desired mutations by restriction digestion and DNA sequencing. Single colonies were picked from the plates, inoculated into 3 mL of LB medium, and grown overnight at 37 °C with shaking at 250

rpm. The plasmids from five ampicillin-resistant single colonies were screened for the presence of the desired mutation by digestion with the *Nde*I restriction enzyme. The pET22b(+):*PDC1* fragment contains only one *Nde*I restriction site and produces a linear fragment upon digestion with *Nde*I. Because one additional *Nde*I restriction site was created by site-directed mutagenesis for the E91A variant, the restriction digestion of pET22b(+):*PDC1-E91A* gives a 6.9 kb fragment and a 0.28 kb fragment. Two of the fragments were identified to have the correct mutation. The mutation was confirmed by DNA sequence analysis using the primer 5′-CCGCGAAATTAATACGACTCACTATA-3′. Cultures of *E. coli* strain BL21(DE3) were transformed with the mutated plasmids for protein overexpression.

Construction of the E91D and E91Q PDC variants was based on the PCR megaprimer method (*22*), which needs two flanking primers, one mutagenic primer, and two rounds of PCR. A pET22b(+) vector containing the *PDC1* gene was used as the template in the PCR. In the first round of PCR, the oligonucleotide 5′-CCGCGAAATTAATACGACTCACTATA-3′ was used as a flanking primer, and oligonucleotides 5′-AACACCGACGTG**AT**CAGCGTAAGAACC-3′ [changed the Glu at position 91 to Asp (bold) and eliminated one A*fl*III restriction site for mutant screening (underlined)] and 5′-AACACCGACGTG**CTG**AGCGTAAGAACC-3′ [changed the Glu at position 91 to Gln (bold) and eliminated one *Afl*III restriction site for mutant screening (underlined)] were used as mutagenic primers. In the second round of PCR, 5′-GTTATGCTAGTTATTGCTCAGCGGT-3′ was used as a flanking primer, and the mutagenic DNA fragment (0.3 kb) produced by the first round was used as a second primer (called megaprimer), giving one 1.8 kb fragment containing the desired mutation. Both the product of the second PCR and the plasmid pET22b(+):*PDC1* were digested by *Xba*I−*Sac*I. The digested reaction mixtures were analyzed on a 0.7% low-melting point agarose gel. The desired fragments [a 1.8 kb mutagenic *PDC1* fragment and a 5.4 kb pET22b(+) fragment] were purified from the gel. The *Xba*I−*Sac*I-digested mutagenic *PDC1* fragment was ligated into the *Xba*I−*Sac*I-digested pET22b(+) fragment. The ligation mixture was transformed into *E. coli* DH5α competent cells. The mutation was screened by digestion with *Afl*III. The pET22b(+):*PDC1* fragment possesses four *Afl*III restriction sites and produces four fragments (3.7, 2.1, 1.1, and 0.28 kb) upon digestion. While one of the *Afl*III restriction sites is destroyed by site-directed mutagenesis in the E91D and E91Q variants, the restriction digestion gives three fragments with sizes of 3.7, 2.1, and 1.4 kb, respectively. The mutations were confirmed by sequence analysis using the same primer that was used for the E91A mutation. Cultures of *E. coli* strain BL21(DE3) were transformed with the mutated plasmids for protein overexpression.

DNA Sequencing. DNA sequence analysis was performed on an ABI 373 DNA Sequencer using dye-labeled dideoxynucleotide terminators. The sequencing reaction was performed using the ABI PRISM Dye Terminator Sequencing Ready Reaction Kit, with AmpliTaq DNA Polymerase, FS, supplied by Applied Biosystems−Perkin-Elmer.

PDC Overexpression and Purification. The *E. coli* BL21(DE3) cells harboring pET22b(+):*PDC1* were used for the expression of the recombinant PDC protein (*23*). The cells were grown in LB medium (containing 100 μg/mL ampicillin, 1 mM thiamin chloride, and 1 mM $MgSO_4$) at 37 °C with shaking. PDC expression was induced in late log phase (OD_{600} = 0.4−0.6) by the addition of 0.2 mM isopropyl β-D-thiogalactopyranoside. The cells were harvested by centrifugation at 8000 rpm and 4 °C for 10 min on a Beckman J2-21 centrifuge (Beckman Instruments). The cells were resuspended in 40 mL of 20 mM potassium phosphate buffer (pH 6.8) containing 1 mM EDTA-2Na, 2 mM $MgSO_4$, 1 mM PMSF, 1 mM ThDP, 5 mM (DTT), and 0.05% (w/v) reduced Triton X-100. The cell suspension was disrupted at 20 kHz in an ice bath for 6 min on a 550 Sonic Dismembrator (Fisher Scientific) and centrifuged at 18 000 rpm and 4 °C for 30 min. The precipitate was discarded, and ammonium sulfate was added to the supernatant to a final concentration of 1.5 M. The solution was stirred at room temperature for 15−30 min and then centrifuged at 18 000 rpm at 4 °C for 15 min. The supernatant was saved, and ammonium sulfate was added to the supernatant to a final concentration of 2.8 M under continuous stirring at room temperature for 15−30 min. The pellet containing the crude enzyme was collected by centrifugation at 18 000 rpm and 4 °C for 15 min. The pellet was resuspended in 3−5 mL of 20 mM Bis-Tris (pH 6.8) containing 1 mM EDTA-2Na, 2 mM $MgSO_4$, 0.5 mM PMSF, and 1 mM ThDP and dialyzed against the same buffer at 4 °C overnight. The desalted enzyme solution was loaded onto a DEAE-FF column (26 cm × 10 cm; on a Pharmacia FPLC system with the FPLC Director computer program) equilibrated with 20 mM Bis-Tris (pH 6.8) containing 1 mM EDTA-2Na, 2 mM $MgSO_4$, and 0.5 mM PMSF. The protein was eluted by a linear gradient with 1 M NaCl at a flow rate of 5.0 mL/min. Fractions (4.0 mL) were collected and were evaluated for protein content and PDC activity, and then checked for purity using SDS−PAGE. The preparation was concentrated to 10−20 mg/mL protein and exchanged into 100 mM potassium phosphate (pH 6.10) containing 1 mM EDTA-2Na, 20 mM $MgSO_4$, 1 mM PMSF, 20 mM ThDP, and 0.05% (w/v) NaN_3 using Amicon Centriprep-30 devices. For long-term storage, glycerol was added to the preparation to a final concentration of 30% (v/v), and the preparation was stored at −20 °C.

The assay for PDC was the NADH/alcohol dehydrogenase-linked coupled assay (*24*).

Steady-state kinetic analysis was carried out at a variety of pH values and assessed as described previously (*7*, *18*, *25*).

Preparation of the Apoenzyme. The PDC enzyme obtained by ion-exchange chromatography (2 mg/mL, 5 mL) was diluted 10-fold with 100 mM Tris/NaOH (pH 8.9), which also contained 1 mM EDTA, and then stirred for 10 min at room temperature. The protein was precipitated by making the solution 2.8 M in ammonium sulfate. The precipitate was resuspended in 0.5 mL of 20 mM Tris/NaOH (pH 8.9) which also contained 1 mM EDTA, and the solution was dialyzed against several changes of the same buffer overnight at 4 °C. The protein was separated from the cofactors by gel filtration on a Superdex 200 column (Pharmacia, 1.0 cm × 30 cm) equilibrated with 100 mM MES/NaOH (pH 6.0).

Thermostability Studies. The purified WT PDC or E91 variant was dialyzed against 50 mM potassium phosphate (pH 6.10) containing 2 mM EDTA, 10 mM $MgSO_4$, 10 mM ThDP, and 0.5 mM PMSF. Next, the total protein concentration was adjusted using the same buffer to 0.5 mg/mL. The

solution was incubated in a polymerase chain reaction thermocycler (MiniCycler, MJ Technologies) for 5 min at the indicated temperature and then stored on ice until assayed for activity on a Varian DMS 300 UV−Visible Spectrophotometer at 25 °C.

ThDP concentrations were measured at room temperature in 100 mM MES (pH 6.0) using a molar extinction coefficient of 8550 M^{-1} cm^{-1} at 267 nm (*26*).

Intrinsic PDC fluorescence was measured on a SLM 8100 spectrofluorimeter in a 0.8 mL quartz cuvette. The excitation wavelength was 300 nm (bandwidth of 4 nm), and the emission spectrum was recorded in the 305−400 nm range (bandwidth of 4 nm). The purified WT PDC or E91 variant was dialyzed against 100 mM MES (pH 6.0) containing 1 mM ThDP and 10 mM $MgSO_4$, and then the total protein concentration was adjusted to 0.1 mg/mL using the same buffer. The extent of binding of ThDP was measured by monitoring the quenching of the apoenzyme intrinsic fluorescence after addition of increments of coenzyme at 25 °C in 0.8 or 3.5 mL quartz cuvettes in 100 mM MES buffer (pH 6.0), with a final concentration of apoenzyme of 0.1 mg/mL. The emission maximum at 338 nm was recorded for each solution. Each emission value was the average of three consecutive measurements. All fluorescence intensity measurements were corrected for the inner-filter effect due to the absorbance of the ThDP by the following formula (*27*)-where F_c and F are the corrected and measured fluorescence

$$F_c = F \text{ antilog}[(A_{ex} + A_{em})/2] \quad (1)$$

intensities, respectively, and A_{ex} and A_{em} are the solution absorbances at the excitation and emission wavelengths, respectively. The quenching data were fitted to the following equations by using the programs KaleidaGraph from Synergy Software (Reading, PA) and DeltaGraph4.0 from DeltaPoint:

$$(\Delta F/F_0 \times 100) = [(\Delta F_{max}/F_0 \times 100)[Q]]/(K_d + [Q]) \quad (2)$$

where $\Delta F/F_0 \times 100$ is the percent quenching (percent change in fluorescence relative to the initial value) following addition of quencher at a concentration [Q] and K_d is the dissociation constant. The modified Stern−Volmer equation (*28*)

$$F_0/(F_0 - F) = 1/(f_a K_{sv}[Q]) + 1/f_a \quad (3)$$

where F_0 is the intrinsic fluorescence of the protein in the absence of quencher, F is the observed fluorescence at quencher concentration [Q], and K_{sv} is the Stern−Volmer collisional quenching constant (determined from the slope of the Stern−Volmer plot at lower concentrations of quencher) can be used to analyze the conformational changes in protein and the accessibility of fluorophore. In this formulation, f_a is the fractional number of accessible fluorophores which was determined from a plot of $F_0/(F_0 - F)$ versus 1/[Q].

Mass Spectrometry. Homogeneous WT PDC and the E91D variant were desalted by gel filtration on a PD-10 column (Pharmacia, 1.5 cm × 5 cm). The enzyme solution (1 μL, 2 mg/mL) was mixed with 1 μL of sinapinic acid. The molecular mass was determined on a Voyager-DE (PerSeptive Biosystems, Inc.) time-of-flight (TOF) mass spectrometer with matrix-assisted laser desorption ionization (MALDI), using bovine serum albumin as the standard.

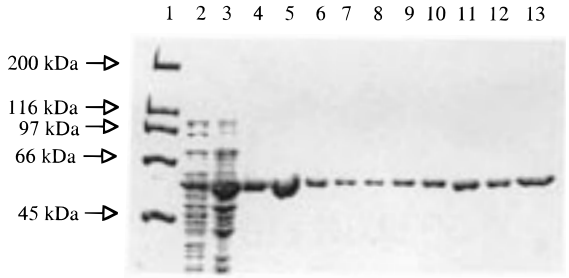

1. High molecular weight standard
2. Crude extract
3. Ammonium sulfate fractionation
4-6. DEAE column fractions of WT PDC
7-9. DEAE column fractions of E91A variant of PDC
10-11. DEAE column fractions of E91D variant of PDC
12-13. DEAE column fractions of E91Q variant of PDC

FIGURE 1: SDS−PAGE analysis for the purification of WT and its E91A, E91D, and E91Q variants. High-molecular mass markers with molecular masses denoted on the left: myosin (200 kDa), β-galactosidase (116.3 kDa), phosphorylase *b* (97.4 kDa), serum albumin (66.2 kDa), and ovalbumin (45 kDa).

Circular dichroism (CD) spectroscopy was carried out at 25 °C on a AVIV model 202 circular dichroism spectrometer equipped with a thermoelectric temperature controller, using 1 mm path length quartz Suprasil cuvettes containing 50 mM potassium phosphate buffer (pH 6.0) and 10 mM $MgSO_4$. Experimental conditions for data collection were as follows: wavelength range, 240−360 nm; repeat, 3; wavelength step, 1 nm; averaging time, 1.0 s; filter setting time, 0.33 s; bandwidth, 1.0 nm; and slit width, 0.043 nm. Data treatment and calculations utilized the AVIV software or the KaleidaGraph program. CD data are presented in units of millidegrees.

RESULTS

Construction of the E91A, E91D, and E91Q Variants of PDC. To investigate the functional importance of glutamic acid 91 in a possible signal transmission pathway from the C221-bound substrate on the β domain to the ThDP, glutamic acid 91 was replaced with alanine (E91A), aspartic acid (E91D), and glutamine (E91Q) via site-directed mutagenesis. The desired mutation in the E91A gene was identified by *Nde*I restriction digestion, and the correct mutations in the E91D and E91Q genes were screened by restriction digestion with *Afl*III. All mutations were confirmed by DNA sequence analysis (*29*). No base change other than that desired was detected.

Expression and Purification. The E91A, E91D, and E91Q variants of PDC were expressed in *E. coli* strain BL21(DE3). Both WT and variants were overexpressed in similar amounts and found in the soluble fraction after cell lysis, and then purified to apparent homogeneity by DEAE anion-exchange chromatography following the same procedure. The purified enzymes migrated as a single band with a molecular mass of 60 000 Da in SDS−PAGE gels (Figure 1). A molecular mass of 61 320.1 ± 60 Da for the WT and 61 223.7 ± 60 Da for the E91D variant was determined by mass spectrometry (MALDI-TOF; *29*). The theoretical molecular mass calculated from the nucleotide sequence of the *PDC1* gene is 61 468 Da.

Scheme 2

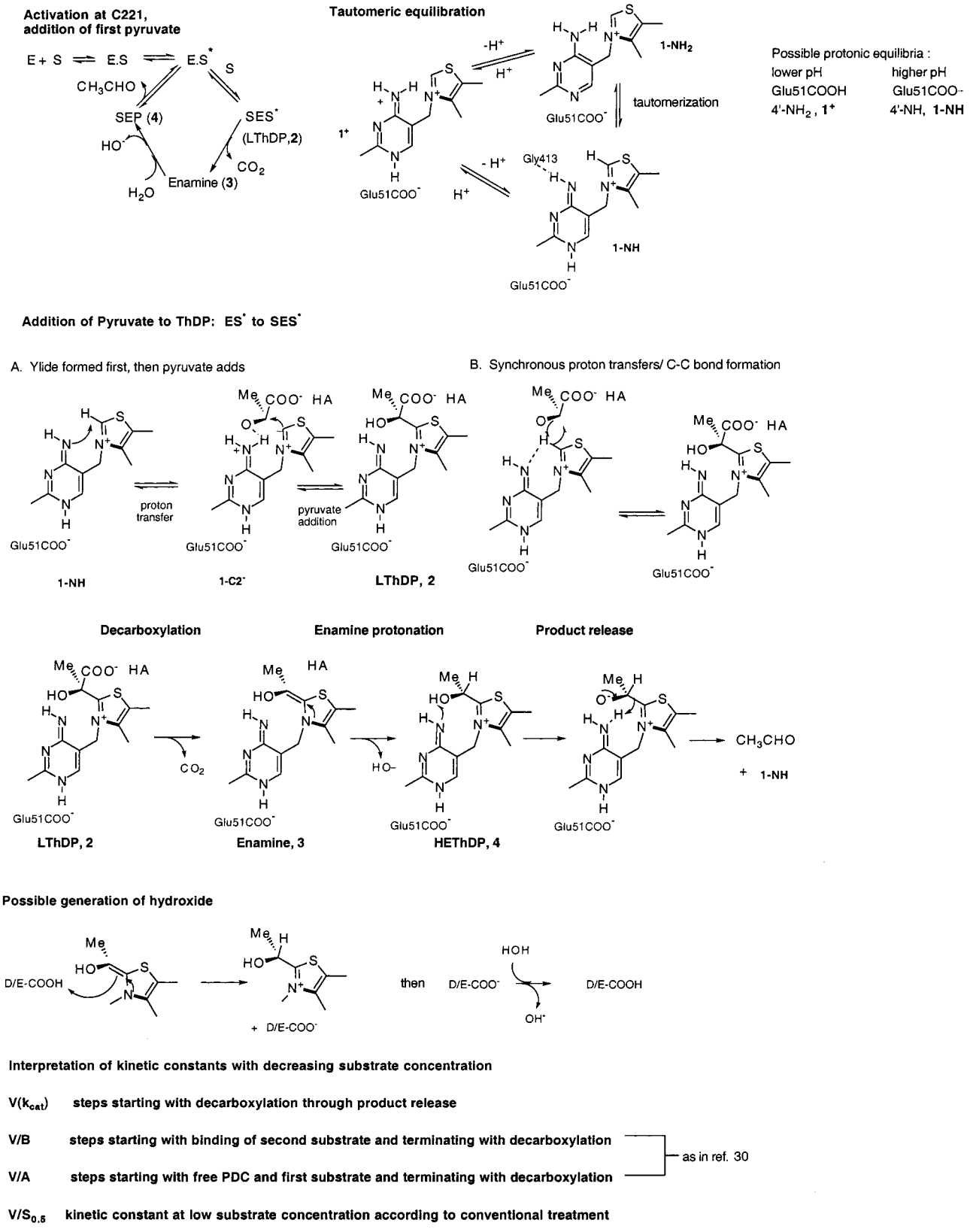

Steady-State Kinetic Analysis of WT and E91 Variants of PDC. The kinetic data were fitted to the Hill equation $\{v_o/E_0 = (k_{cat}S^n)/[(S_{0.5})^n + S^n]\}$, and the parameters were determined from a linear least-squares fit. The data were also treated according to the mechanism depicted in Scheme 2, upper left, specific to PDC, and assuming two pyruvate sites, one regulatory and one catalytic, as developed by Schowen and collaborators (*30*):

$$v_o = V_{max}S^2/(A + BS + S^2) \quad (4)$$

from which instead of the conventional V_{max}, K_m, and $V_{max}/$

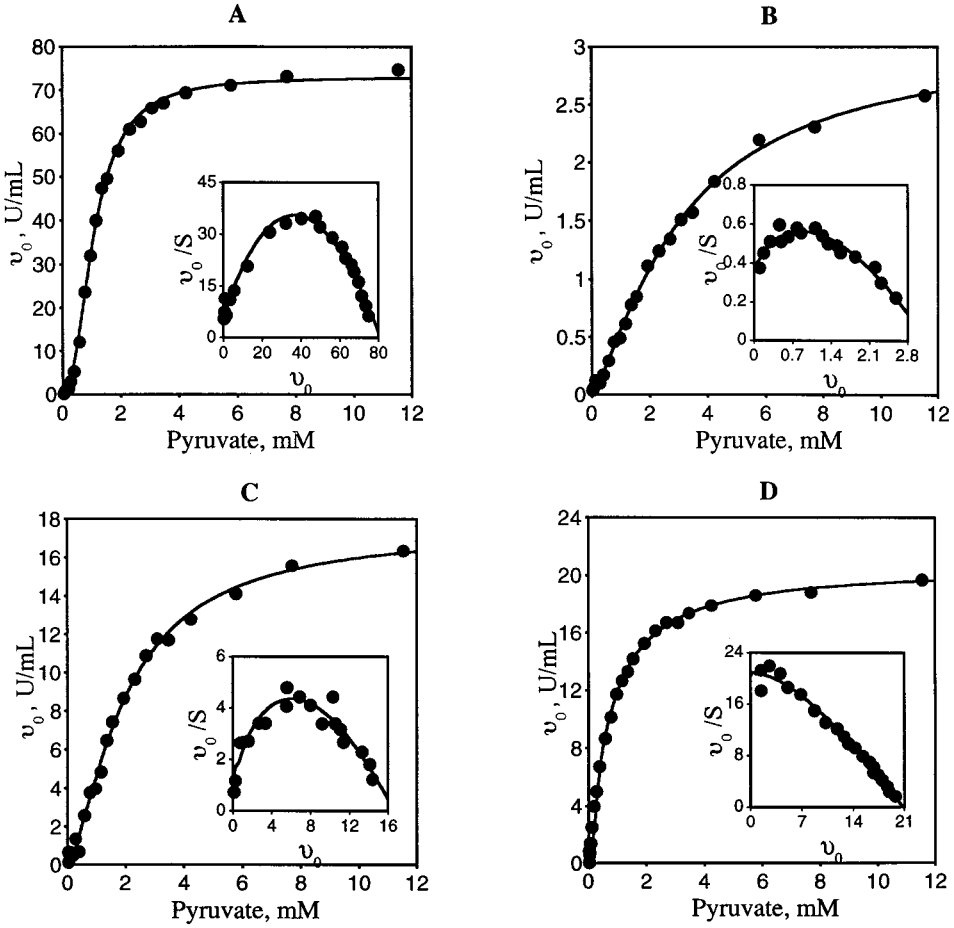

FIGURE 2: v_o-S plots for WT (A) and the E91A (B), E91D (C), and E91Q (D) variants. Experiments were carried out in 100 mM MES at pH 6.0 and 25 °C. The insets are Eadie−Scatchard plots.

Table 1: Comparison of the Steady-State Kinetic Parameters of WT and E91 Variants of PDC in 0.1 M MES Buffer at pH 6.0 and 25 °C

	specific activity (units mg^{-1})	$S_{0.5}$ (mM)	k_{cat} (s^{-1})	$k_{cat}/S_{0.5}$ (mM^{-1} s^{-1})	n_H
WT	60 ± 5	1.09 ± 0.17	73.1 ± 1.4	67.1 ± 9.4	2.18 ± 0.05
E91A	2.0 ± 0.2	4.70 ± 0.19	3.1 ± 0.5	0.65 ± 0.09	1.31 ± 0.05
E91D	11 ± 1	1.79 ± 0.22	17.5 ± 0.2	9.81 ± 1.08	1.86 ± 0.14
E91Q	16 ± 1	0.89 ± 0.02	20.4 ± 0.2	22.95 ± 0.23	1.09 ± 0.02

K_m (for the current substrate-activated case, V_{max}, $S_{0.5}$, and $V_{max}/S_{0.5}$), the constants V_{max}, V_{max}/B, and V_{max}/A are deduced (and if accurate enzyme concentrations are known, k_{cat}, k_{cat}/B, and k_{cat}/A, corresponding to a collection of rate constants that are zero-, first-, and second-order in S). Representative v_o-S plots for WT and E91 variants at pH 6.0 are shown in Figure 2, with the Eadie−Scatchard plots in the inserts. The derived steady-state kinetic parameters at pH 6.0 are presented in Table 1. At this pH, the specific activities decreased in the following order: WT > E91Q ≥ E91D ≫ E91A (4-, 5-, and 30-fold, respectively); the turnover numbers (k_{cat}) decreased in the same fashion. At pH 6.0, the $S_{0.5}$ changed little in the E91D and E91Q variants, but exhibited a 4.5-fold increase for the E91A variant, a result of a shift in the $S_{0.5}$−pH plots. The catalytic efficiency ($k_{cat}/S_{0.5}$) decreased in the same order as the specific activity. While the Hill coefficient of the E91D variant was nearly as large as that of WT, it was very much reduced in the E91A and E91Q variants.

Table 2: Apparent pK_a Data for WT and Its E91A, E91D, and E91Q Variants Estimated from pH-Dependent Kinetic Parameters[a]

	WT		E91A		E91D		E91Q	
kinetic constant	pK_{a1}	pK_{a2}	pK_{a1}	pK_{a2}	pK_{a1}	pK_{a2}	pK_{a1}	pK_{a2}
k_{cat}	5.4	7.0	5.8	6.5	5.4	6.7	5.5	6.3
$k_{cat}/S_{0.5}$	5.3	6.5	ND[b]	6.1	ND[b]	6.0	5.4	6.3
V/A	5.5	6.5	ND[b]	6.4	ND[b]	6.0	ND[b]	ND[b]
V/B	ND[b]	ND[b]	ND[b]	6.4	5.5	6.5	5.41	6.30

[a] The results were obtained from both semilog (kinetic constant−pH) and log−log [log(kinetic constant)−pH] plots; pK_{a1} and pK_{a2} refer to the apparent values determined on the acid and alkaline side of the curves, respectively. The estimated error is ±0.3 unit on fitting the data from Tables S1−S4 and Figures S1−S4 to a Dixon−Webb equation by a nonlinear least-squares method. [b] No values could be estimated from the data due to the absence of an apparent pH dependence in the pH range that was examined, or the pH dependence not being readily interpretable.

The pH dependence of steady-state kinetic parameters was determined for WT and for the E91D, E91Q, and E91A variants and is summarized in Figures S1−S4 and Tables S1−S4 in the Supporting Information. The values of pK_{app} deduced from the shapes of the kinetic curves are shown in Table 2. The substitutions at position 91 in PDC resulted in significant perturbations in several parameters. The shapes of k_{cat} versus pH for WT and the E91 variants are similar, but the two pK_{app} values are closer to each other for the E91 variants; i.e., the bell-shaped curves are much narrower. Compared to those of WT, the $k_{cat}/S_{0.5}$ versus pH curves for all E91 variants are shifted to lower pH by at least 0.4−0.5

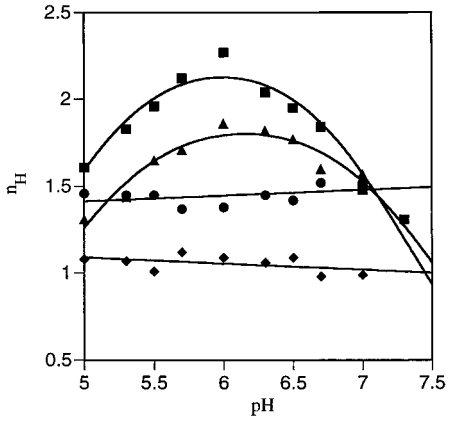

FIGURE 3: pH dependence of the Hill coefficient for WT and its E91 variants: WT PDC (■), E91A (●), E91D (▲), and E91Q (◆).

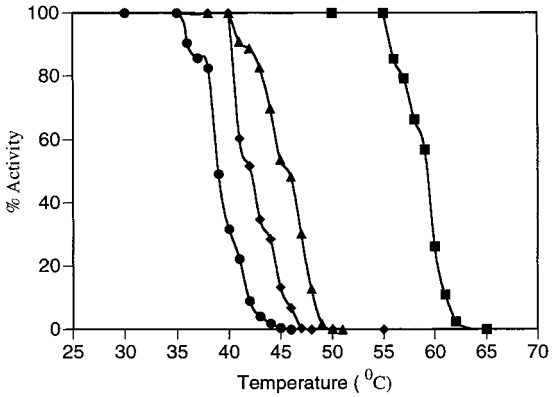

FIGURE 4: Thermostability of WT and its E91 variants: WT (■), E91A (●), E91D (▲), and E91Q (◆).

pH unit, with the maximum values at pH ~5.5, whereas the *V*/*B* versus pH plots are shifted to the alkaline region by 0.5 pH unit for the E91 variants. The most striking differences are observed in the Hill coefficients. The Hill coefficients for the WT PDC and the E91D variant exhibit a pronounced pH dependence with the maximum at pH ~6.0, while those for the E91Q and E91A variants are almost pH-independent (Figure 3).

Thermostability. To test the effect of substitution at position 91 on the tertiary structure, the thermostability of the WT and E91 variants was studied under the same experimental conditions (Figure 4). The thermostability of all E91 variants was significantly reduced compared to that of the WT. The T_m for WT PDC was 59.5 °C, while the T_m values were reduced by 14 °C for the E91Q, 17 °C for the E91D, and 21 °C for the E91A variants.

Intrinsic Fluorescence Measurements. The intrinsic fluorescence emission spectra of WT PDC and the E91 variants are shown in Figure 5. The E91D variant has the same fluorescence emission maximum at 328 nm as the WT PDC upon excitation at 300 nm, while the fluorescence emission maximum of the E91A is red-shifted by 5 nm (333 nm) and that of E91Q by 3 nm (331 nm).

Relative Cofactor Binding. For WT PDC, less than 1% activity was obtained when the apoenzyme was assayed without added cofactors [ThDP and Mg(II)] compared to the fully reconstituted enzyme. This confirms that the experiment successfully removed both cofactors. However, the enzyme fully reconstituted with saturating ThDP and Mg(II) has only 87−95% of the activity of the native enzyme, showing some loss of catalytic activity during resolution of cofactors in producing the apo-PDC. For all the E91 variants, the cofactors could be separated by DEAE anion-exchange chromatography at pH 6.8; therefore, the E91 variants were purified as apoenzymes. Full catalytic activity could be recovered after the mutant enzymes were preincubated with 10 mM $MgSO_4$ and 10 mM ThDP in 100 mM potassium phosphate (pH 6.0) for 30 min at 25 °C. Binding constants for binding of the cofactors to the native apoenzyme and apo-E91 variants were determined from the quenching of intrinsic fluorescence on addition of increasing concentrations of cofactor to the apoenzymes in the presence of saturating concentrations of the second cofactor at pH 6.0 (Figure 5). The enzyme exhibits a fluorescence emission maximum at 338 nm upon excitation at 290 nm, suggesting that it very likely corresponds to a buried tryptophan in PDC (*31*). The quenching of apo-PDC fluorescence by cofactors is concentration-dependent and saturable, following a typical hyperbolic binding curve (data not shown). The values of K_d and the percent quenching were extracted for low and high concentrations of ThDP (Table 3), indicating that the affinity of the E91D, E91Q, and E91A variant apoenzymes for ThDP·Mg(II) decreased significantly compared to that of WT.

Circular Dichroism Measurements. While ThDP alone has no optical activity, upon binding to the native apoenzyme, it experienced a distinct spectral change. Two new peaks were induced with characteritsic maxima at 263 and 283 nm, as previously reported by Killenberg-Jabs and co-workers (*32*). All three E91 variants exhibited significant differences in their near-UV CD spectra with respect to those of the WT, although the CD spectra of the four apoenzymes were very similar (Figure 6). For all the E91 variants, the minimum at 283 nm almost disappeared, and the CD signal could not be observed even in the presence of a great excess of ThDP. The maximum at 263 nm exhibited a distinct broadening, as well as being shifted to shorter wavelengths in the spectra of the variants.

DISCUSSION

As can seen in Figure 7, the side chain of E91 makes numerous van der Waals contacts with the short loop in the γ domain comprising residues 410−415 leading to the active site, including a hydrogen bond from the E91 side chain to the main chain nitrogen of W412. It needs to be emphasized that all of the residues examined so far on the putative substrate-activation pathway emanating from C221 (C221, H92, and E91) are on the same subunit, albeit on different domains. The last three residues of this segment (413−415 also on the same subunit) provide some of the key conserved interactions between ThDP enzymes and ThDP, while residues 410−412 are connected to the regulatory site pocket through direct and indirect interactions with E91. Therefore, substitutions at E91 are expected to cause significant perturbations in the substrate activation process and the active site, as reflected by steady-state kinetics, thermostability, cofactor binding, and tertiary structural changes of the enzyme. The E91 variants could be purified by the same protocol optimized for the WT PDC (*33*), although the variant enzymes were purified as apoenzymes. It is reasonable to conclude that the variants folded in the correct

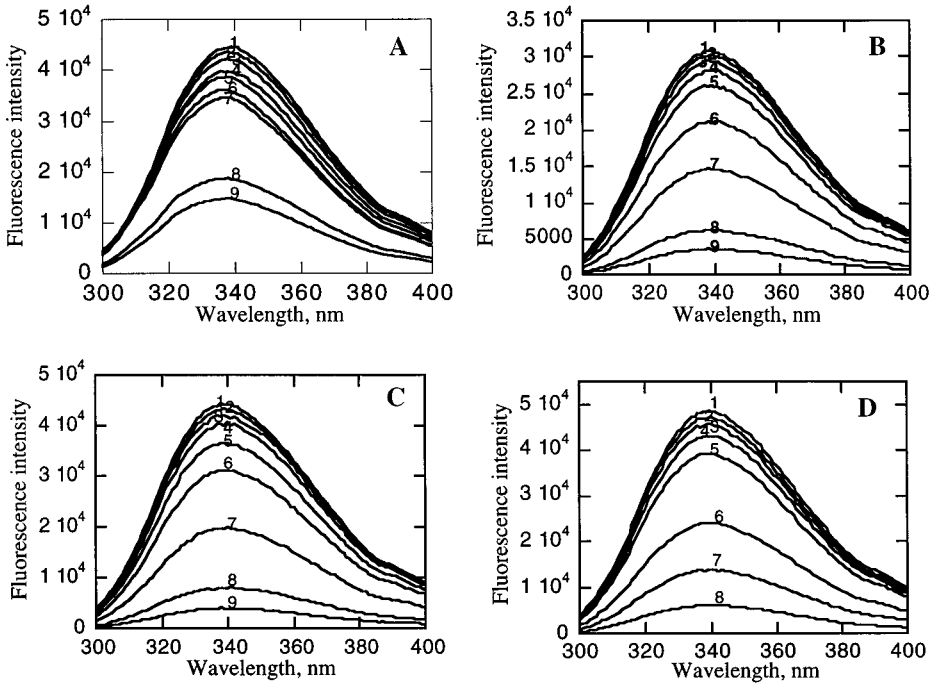

FIGURE 5: (A) Effect of ThDP on the tryptophan fluorescence emission spectrum of WT. The enzyme (0.1 mg/mL) was preincubated with 10 mM Mg(II) in 100 mM MES (pH 6.0), and then the following concentrations of ThDP were added: (1) 0, (2) 1.55, (3) 3.10, (4) 6.20, (5) 12.38, (6) 24.74, (7) 30.90, (8) 162.93, and (9) 228.81 μM. (B) Effect of ThDP on the tryptophan fluorescence emission spectrum of E91A PDC. The enzyme (0.1 mg/mL) was preincubated with 10 mM Mg(II) in 100 mM MES (pH 6.0), and then the following concentrations of ThDP were added: (1) 0, (2) 2.78, (3) 8.35, (4) 16.68, (5) 33.29, (6) 68.30, (7) 156.65, (8) 362.12, and (9) 508.31 μM. (C) Effect of ThDP on the tryptophan fluorescence emission spectrum of E91D PDC. The enzyme (0.1 mg/mL) was preincubated with 10 mM Mg(II) in 100 mM MES (pH 6.0), and then the following concentrations of ThDP were added: (1) 0, (2) 2.78, (3) 8.35, (4) 16.68, (5) 33.29, (6) 69.52, (7) 161.50, (8) 375.43, and (9) 527.62 μM. (D) Effect of ThDP on the tryptophan fluorescence emission spectrum of E91Q PDC. The enzyme (0.1 mg/mL) was preincubated with 10 mM Mg(II) in 100 mM MES (pH 6.0), and then the following concentrations of ThDP were added: (1) 0, (2) 5.57, (3) 11.13, (4) 22.22, (5) 44.33, (6) 136.31, (7) 258.67, and (8) 472.01 μM. The wavelength of excitation was 290 nm.

Table 3: Parameters for Quenching the Intrinsic Fluorescence of Apo-WT and Its E91 Variants upon Addition of Cofactors

	apparent K_d (μM)	maximal quenching (%)	f_a
WT	$20.6 \pm 5.5^{a,b}$	$29.1 \pm 6.9^{a,b}$	$0.29 \pm 0.07^{a,b}$
	22.4 ± 2.8^{c}	26.2 ± 2.0^{c}	0.31 ± 0.02^{c}
E91A	2.7 ± 0.2^{a}	2.8 ± 0.1^{a}	0.03 ± 0.00^{a}
	264 ± 86^{b}	59.9 ± 22.8^{b}	0.60 ± 0.23^{b}
E91D	8.4 ± 2.1^{a}	6.7 ± 1.3^{a}	0.07 ± 0.01^{a}
	259 ± 86^{b}	69.9 ± 26.8^{b}	0.67 ± 0.26^{b}
E91Q	29.5 ± 57.9^{a}	11.6 ± 20.3^{a}	0.12 ± 0.20^{a}
	279 ± 97^{b}	67.2 ± 28.5^{b}	0.67 ± 0.28^{b}

[a] Values obtained with 1−12 μM ThDP. [b] Values obtained with 12−500 μM ThDP. [c] Values obtained with 1−12 μM Mg(II).

conformation, consistent with the finding that all E91 variants are able to bind the cofactors and exhibit varying levels of activity.

Effects of Substitution at E91 on Steady-State Kinetic Parameters and Their pH Dependence. Hill Coefficient. The most telling kinetic parameter undergoing the most dramatic changes with substitution of E91 is the Hill coefficient; it is 2.2−1.8 for WT and E91D, and it is reduced to 1.1−1.3 for E91A and E91Q. These results support the hypothesis that E91 is on the information transfer pathway during the substrate activation process. The E91D variant, with the negative charge conserved, results in an active enzyme with a Hill coefficient of 1.8−1.9, suggesting that the negative charge at position 91 is very important in maintaining the activity and cooperativity. Although the E91A and E91Q variants are unstable under the normal storage conditions compared to the WT, with loss of most of the activity and cooperativity within 1 week, the E91D variant is relatively stable with little change in activity and cooperativity within 1 week, also supporting the hypothesis. This hypothesis is also supported by the results that the Hill coefficients for WT and E91D variant are pH-dependent and their curves are bell-shaped with the maximum at pH ~6.0, while those for the E91A and E91Q variants are nearly pH-independent. Elsewhere, we suggested that the ascending part of the curve is due to ionization of C221 ($pK_a \sim 5.2$), and the descending part to H92 ($pK_a \sim 6.4$). It is interesting to note that several of the interactions identified among domains and subunits in PDC tend to involve at least one charged residue as seen here, and in some cases two, as seen in the $C221S^{-}H^{+}H92$ ion pair (*19*), implying that the forces responsible for these interactions are electrostatic in origin. The substitution of E91 with A leads to great reduction in both activity and cooperativity. In contrast, the E91Q variant has a dramatic effect only on the Hill coefficient rather than on the activity and $S_{0.5}$. This comparison suggests that the length of the side chain at position 91 is also very important in both substrate binding and catalysis of the enzyme; i.e., the side chain Q can still form a hydrogen bond with W412, but apparently, the initial velocity of this variant no longer responds to substrate concentration in a sigmoidal manner. This could be the result of one of two scenarios; either the E91Q variant can no longer be activated, or it exists in its activated form. The low values of $S_{0.5}$ suggest the latter possibility.

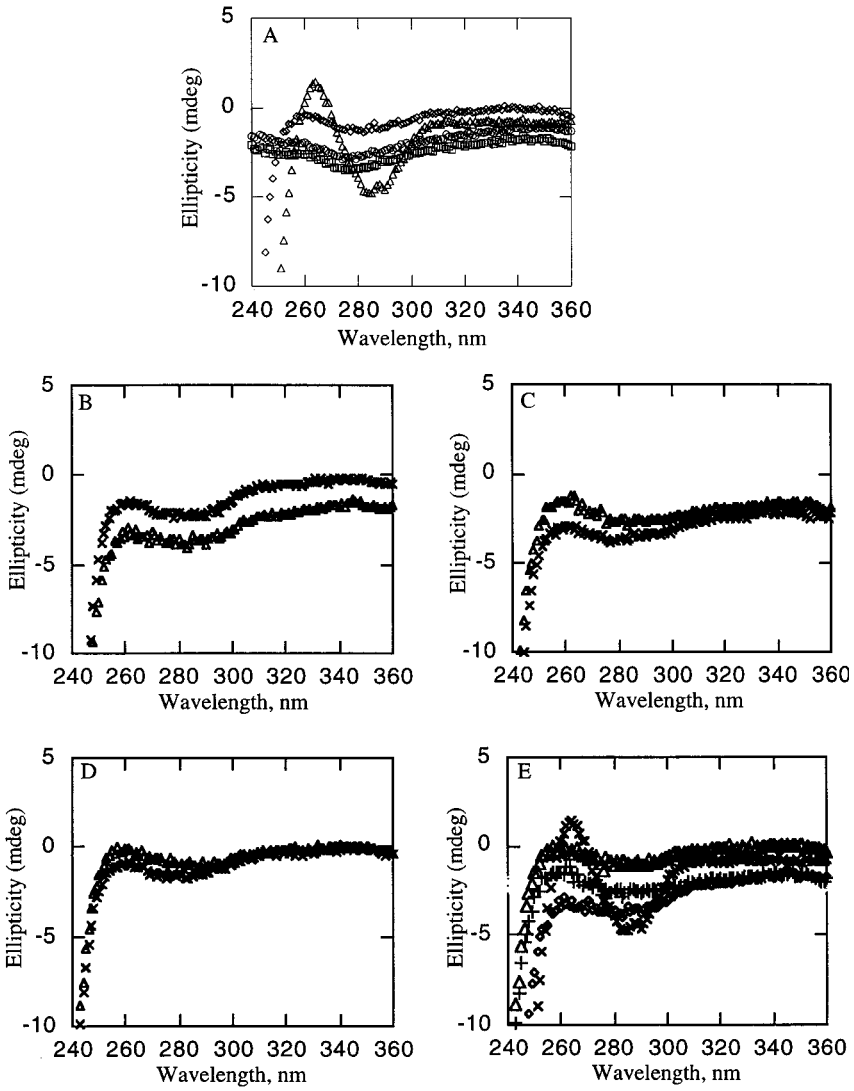

FIGURE 6: Near-UV CD spectra of PDC and its E91 variants in the absence and presence of ThDP. (A) WT: apoenzyme (◇), apoenzyme and 0.1 mM ThDP (△), 0.1 mM ThDP (○), and 50 mM phosphate (pH 6.0) (□). (B) E91A PDC: apoenzyme (×) and apoenzyme and 1 mM ThDP (△). (C) E91D PDC: apoenzyme (×) and apoenzyme and 1 mM ThDP (△). (D) E91Q PDC: apoenzyme (×) and apoenzyme and 1 mM ThDP (△). The apoenzyme (2 mg/mL) was preincubated with 10 mM Mg(II) in 50 mM potassium phosphate at pH 6.0 and 25 °C. Then the ThDP was added, and the spectra were recorded with a path length of 0.1 cm. (E) Composite of all four forms with 1 mM ThDP each: WT (×), E91A (◇), E91D (+), and E91Q (△).

pH Dependence of the Steady-State Parameters. In the Dixon−Webb formalism, apparent pK_a values that modulate V and $V/S_{0.5}$ pertain to protonic equilibria involving the E·S complex and free E, respectively. According to the mechanism derived by Alvarez et al. (*30*), V_{max}/A reflects on the energetics of transition states starting with the addition of the first pyruvate to PDC (presumably at the regulatory site, very likely C221) and terminating with the first irreversible step, i.e., decarboxylation. The term V_{max}/B reflects the energetics of transition states starting with the E·S complex and terminating with decarboxylation. Finally, V_{max} (or k_{cat}) reports on transition-state energies for the decarboxylation step (formation of the enamine or 2-α-carbanion), followed by product release (broadly defined), including protonation of the enamine and release of acetaldehyde from ThDP (Scheme 1). In turn, the pK_a values implied by the V/A−pH plots refer to free enzyme (i.e., at [S] ≪ S_0), those from the V/B−pH plots to PDC·S_R with a substrate bound at the regulatory site (C221; at [S] ≪ S_0), and finally those from V−pH (or k_{cat}−pH) plots to S_C·PDC·S_R with substrate bound at both the catalytic and regulatory sites (at [S] ≫ S_0).

Behavior of $S_{0.5}$. It is important to note that $S_{0.5}$ in all cases studied to date is reduced as the solution becomes more acidic, irrespective of whether it represents the true K_m (i.e., n_H is 1.0). This suggests that the affinity for pyruvate at both the regulatory and catalytic centers is more favorable at lower pH (compare, for example, the WT and the E91Q variant), presumably reflecting the charge on the substrate and the sites. At higher pH, both C221 and the active center with its E477 and D28 would be expected to develop negative charges, accounting for this pH dependence.

Behavior of V or k_{cat} versus pH. The k_{cat}−pH profiles are bell-shaped for WT and E91 variants, suggesting that at least one ionizable side chain contributes to catalysis on both sides of the profile. The values of pK_{app} are closer to each other in the variants than in the WT, implying that there is some perturbation in the values of pK_{app} in the active site residues, even though the substitutions do not influence significantly

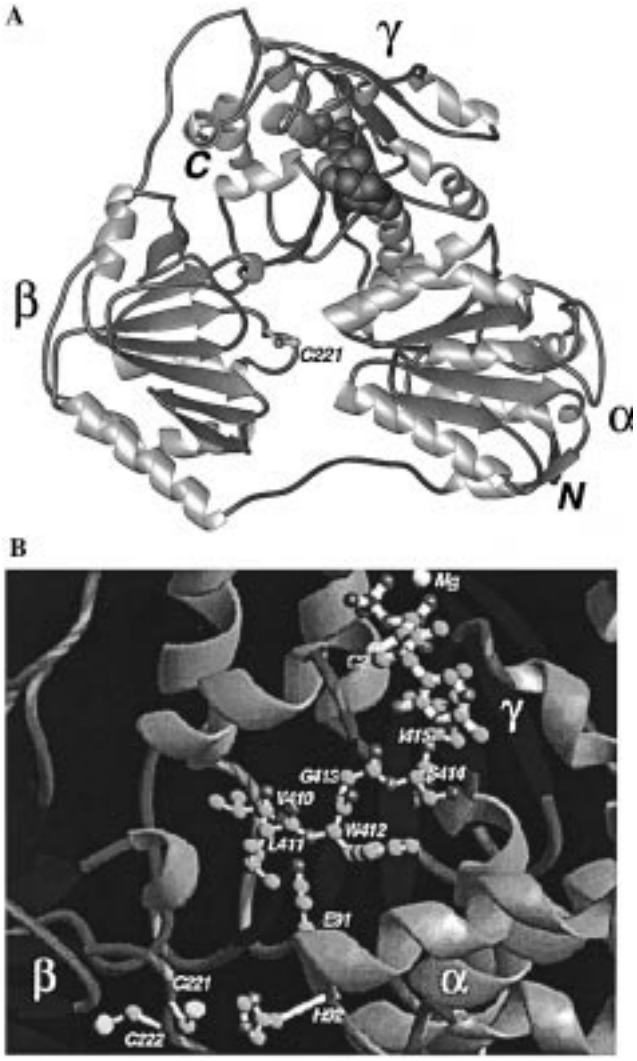

FIGURE 7: (A) Ribbon diagram of a yeast PDC monomer showing the location of C221 with respect to the thiamin diphosphate (in space-filling format). (B) The putative substrate activation pathway emanating from C221 to H92 to E91 to W412 to G413 and to ThDP.

the active site of the enzyme, as reflected by the activities.

Behavior of $k_{cat}/S_{0.5}$ and V/A versus pH. The $V_{max}/S_{0.5}$−pH plots have virtually the same shape as the V_{max}/A−pH plots, and both are bell-shaped for the WT, again suggesting that at least one ionizable group on both the acid and alkaline side is involved in the rate-limiting step at low substrate concentrations. The pH optima of the $k_{cat}/S_{0.5}$−pH (or V/A−pH) plots for the E91 variants are shifted to the acidic region by approximately 0.5 pH unit, implying that the pK_a values of the free enzyme are being shifted by the substitutions, probably in the vicinity of C221 or H92. These shifts can be attributed in large measure to the term in the denominator of the kinetic constant (see the pH-dependent behavior of $S_{0.5}$ above).

Behavior of V/B versus pH. In contrast to the acid shift of the $k_{cat}/S_{0.5}$−pH (or V/A−pH) plots, the pH optima of the V/B plots for all E91 variants experience an alkaline shift by perhaps as much as 0.3−0.5 pH unit. This provides strong evidence that different ionizable groups are responsible for the acid limbs of the V/A and V/B profiles and, of course, that substitutions at E91 are sensed at both the regulatory and the catalytic centers as reflected by the shifts in the apparent pK_a values. The pK_a values sensed by the V/B term under acidic conditions must apply to some active center residue(s).

Changes in Tertiary Structure with E91 Substitutions. PDC exhibits intrinsic fluorescence characteristic of the presence of tryptophan residues, very likely buried in the protein as revealed by a low fluorescence emission maximum (338 nm) upon excitation at 290 nm (*31*). The fluorescence emission maximum of the E91A or E91Q variant is red-shifted compared to that of WT PDC upon excitation at 300 nm, implying that a conformational change brings the tryptophan(s) to a less nonpolar (more solvent-accessible) environment. The quenching of tryptophan fluorescence provides a direct tool for the determination of the dissociation constant of a protein−ligand complex. However, the sensitivity of the method depends on the number and location of the fluorophores. It had been reported that the binding of ThDP to the PDC apoenzyme quenches the intrinsic tryptophan fluorescence (*34*−*36*), suggesting that there is a tryptophan in the ThDP binding site (active site). The residue responsible for the source of the fluorescence quenching upon adding cofactors was identified as W487 in *Zymomonas mobilis* PDC (corresponding to W493 in yeast PDC) by site-directed mutagenesis (*37*). This tryptophan residue is also conserved in all known PDCs. It was suggested that there was a direct interaction between this tryptophan and ThDP (*37*). Surprisingly, the crystal structure of yeast PDC showed that this residue is some distance from the active site [11.6 Å from the Mg(II)], but lies at the dimer interface (*14*, *15*). It was then proposed that an alteration of the ring stacking between W493 and F502 of the other subunit is the source of the fluorescence quenching when the ThDP binds to the apoenzyme (*14*). However, the F502 is not absolutely conserved. Recently, it was reported that the F502L and F502H substitutions in *Z. mobilis* PDC did not eliminate the fluorescence quenching upon addition of the ThDP (*38*), thereby ruling out the suggestion that ring stacking with Phe is responsible for the observed fluorescence quenching.

In the presence of ThDP or Mg(II), the Stern−Volmer plots are not upwardly curved (downward-curving plots for WT, and nearly linear plots for all E91 variants), suggesting the existence of only collisional quenching (*39*, *40*). The bimodal behavior for double-reciprocal plots of eq 2 and of the modified Stern−Volmer plots suggests that quenching of fluorescence by cofactors is highly affected by their concentrations, giving linear plots for the low and high concentration ranges. The fraction of residues accessible to fluorescence quenching (f_a = 0.38) for ThDP in WT suggested the participation of only one type of tryptophan residue with similar exposure and accessibility to ThDP. The affinity for ThDP is decreased 10-fold for the E91 variants compared to that of WT, suggesting that the substitutions at E91 induce a conformational change leading to loosening of binding. The marked conformational change induced by cofactor binding is also seen in the variation in quencher accessibility (f_a). Substitution at E91 strongly increased the accessibility to ThDP. For the E91 variants, there is an increase in the accessible fraction from 0.4 to 0.6−0.7, confirming that the environment of tryptophan becomes less hydrophobic. The fluorescence emission maximum is shifted to shorter wavelengths when the cofactors are bound to the apoenzyme in WT PDC, consistent with the internal and

hydrophobic environment of the tryptophan 493. In contrast, the binding of ThDP to the E91 variant apoenzymes induces a relatively large decrease in the intrisic fluorescence (the maximum percent quenching is doubled compared to that of WT) without changing the emission maximum wavelength, suggesting that ThDP binding may induce a distant conformational change of the enzyme which indirectly alters the tryptophan fluorescence, as suggested in the case of HIV reverse transcriptase (*41*).

CD provides an additional tool for monitoring significant differences in the tertiary strctural packing of amino acid side chains in WT and variant enzymes. CD spectra have been used previously for ThDP-dependent enzymes: transketolase (*42*−*44*), pyruvate dehydrogenase (*45*, *46*), yeast PDC (*32*, *47*, *48*), and *Z. mobilis* PDC (*38*). The CD spectra of WT PDC from different sources are similar. The CD signal observed in transketolase is stronger than that of PDC due to the presence of aromatic residues in the cofactor binding pocket in transketolase (missing in PDC), which may form a charge-transfer complex with ThDP (*44*, *49*).

As seen from the CD spectra, ThDP alone has no optical activity; however, addition of ThDP to the WT apoenzyme induces two distinct peaks, a positive maximum at 263 nm, a negative maximum at 283 nm, and a negative diffuse band between 300 and 340 nm. The "induced optical activity" is thought to be due to the binding of ThDP to an asymmetric environment in the protein (*44*, *47*, *48*). In contrast, CD spectra for the E91 variants were moved upward upon addition of ThDP to the apoenzyme, and both peaks exhibit extensive broadening and diffusion. Interestingly, although substitution of E91 with D, which retains the negative charge but shortens the side chain, shows the least effect on the activity and cooperativity of the enzyme, the CD spectra for E91D appear to be similar to those of the other two E91 variants. The results suggest the following: (1) Substitutions at E91 cause conformational changes in the cofactor binding pocket (active site), as well as in the entire enzyme; (2) different tertiary structural change is being induced by ThDP binding to WT than by binding to the E91 variants; (3) the typical CD spectrum induced by ThDP binding to the WT is not absolutely required for catalytic activity and cooperativity of the enzymes.

The tertiary structural changes due to substitutions at E91 have also been confirmed by the fact that the thermostability of E91 variants is significantly decreased. If the inherent interactions between the E91 and the loop of residues 410−415 are important for substate activation and catalysis, the substitutions at E91 must break or weaken these noncovalent bonds, resulting in a local and a more global conformational change of the enzyme.

The results here provide convincing evidence that further supports the proposed substrate activation pathway in yeast PDC: from C221 to H92 to E91 to W412 to G413 to N4′H (ThDP). We conclude that residue E91 can indeed relay the regulatory information from the regulatory site to the active site. Defining the role of the next amino acid W412 in this putative pathway in the accompanying paper provides further valuble insight into the substrate activation mechanism and domain−domain interactions in PDC.

SUPPORTING INFORMATION AVAILABLE

Data tables (Tables S1−S4) and corresponding kinetic curves at different pH values (Figures S1−S4) for WT PDC and its E91A, E91Q, and E91D variants. This material is available free of charge via the Internet at http://pubs.acs.org.

REFERENCES

1. Krampitz, L. O. (1969) *Annu. Rev. Biochem. 38*, 213−240.
2. Sable, H. Z., and Gubler, C. J., Eds. (1982) Thiamin: twenty years of progress, *Ann. N.Y. Acad. Sci. 378*, 7−122.
3. Kluger, R. (1987) *Chem. Rev. 87*, 863−876.
4. Schellengerberger, A., and Schowen, R. L., Eds. (1988) *Thiamin Pyrophosphate Biochemistry*, Vol. 1−2, CRC Press, Boca Raton, FL.
5. Bisswanger, H., and Ullrich, J., Eds. (1991) *Biochemistry and Physiology of Thiamin Diphosphate Enzymes*, pp 1−453, VCH, Weinheim, Germany.
6. Bisswanger, H., and Schellenberger, A., Eds. (1996) *Biochemistry and Physiology of Thiamin Diphosphate Enzymes*, pp 1−599, A. u. C. Intemann, Wissenschaftlicher Verlag, Prien, Germany.
7. Jordan, F., Nemeria, N., Guo, F., Baburina, I., Gao, Y., Kahyaoglu, A., Li, H., Wang, J., Yi, J., Guest, J., and Furey, W. (1998) *Biochim. Biophys. Acta 1385*, 287−306.
8. Muller, Y., Lindqvist, Y., Furey, W., Schulz, G., Jordan, F., and Schneider, G. (1993) *Structure 1*, 95−103.
9. Boiteux, A., and Hess, B. (1970) *FEBS Lett. 9*, 293−296.
10. Hübner, G., Weidhase, R., and Schellenberger, A. (1978) *Eur. J. Biochem. 92*, 175−181.
11. Schellenberger, A., Hübner, G., and Sieber, M. (1988) in *Thiamin Pyrophosphate Biochemistry* (Schellenberger, A., and Schowen, R. L., Eds.) pp 113−121, CRC Press, Boca Raton, FL.
12. Hübner, G., König, S., and Schellenberger, A. (1988) *Biomed. Biochim. Acta 47*, 9−18.
13. Hohmann, S., and Cederberg, H. (1990) *Eur. J. Biochem. 188*, 615−621.
14. Dyda, F., Furey, W., Swaminathan, S., Sax, M., Farrenkopf, B., and Jordan, F. (1993) *Biochemistry 32*, 6165−6170.
15. Arjunan, D., Umland, T., Dyda, F., Swaminathan, S., Furey, W., Sax, M., Farrenkopf, B., Gao, Y., Zhang, D., and Jordan, F. (1996) *J. Mol. Biol. 256*, 590−600.
16. Zeng, X., Farrenkopf, B., Hohmann, S., Dyda, F., Furey, W., and Jordan, F. (1993) *Biochemistry 32*, 2704−2709.
17. Baburina, I., Gao, Y., Hu, Z., Jordan, F., Hohmann, S., and Furey, W. (1994) *Biochemistry 33*, 5630−5635.
18. Baburina, I., Li, H., Bennion, B., Furey, W., and Jordan, F. (1998) *Biochemistry 37*, 1235−1244.
19. Baburina, I., Moore, D. J., Volkov, A., Kahyaoglu, A., Jordan, F., and Mendselsohn, R. (1996) *Biochemistry 35*, 10249−10255.
20. Baburina, I., Dikdan, G., Guo, F., Tous, G. I., Root, B., and Jordan, F. (1998) *Biochemistry 37*, 1245−1255.
21. Papworth, C., Greener, A., and Braman, J. (1995) *Strategies Mol. Biol. 7*, 4−6.
22. Sarkar, G., and Sommer, S. S. (1990) *BioTechniques 8*, 404−407.
23. Studier, F. W., and Moffatt, B. A. (1986) *J. Mol. Biol. 189*, 113−130.
24. Holzer, H., Schultz, G., Villar-Palasi, C., and Jutgen-Sell, J. (1956) *Biochem. Z. 327*, 331−344.
25. Guo, F., Zhang, D., Kahyaoglu, A., Farid, R. S., and Jordan, F. (1998) *Biochemistry 37*, 13379−13391.
26. Wittorf, J. H., and Gubler, C. J. (1970) *Eur. J. Biochem. 14*, 53−60.
27. Lakowicz, J. R. (1983) *Principles of Fluorescence Spectroscopy*, Plenum Press, New York.
28. Lehrer, S. S. (1971) *Biochemistry 10*, 3254−3263.
29. Li, H. (1999) Ph.D. Thesis, Rutgers University Graduate Faculty, Newark, NJ.
30. Alvarez, F. J., Ermer, J., Hübner, G., Schellenberger, A., and Schowen, R. L. (1991) *J. Am. Chem. Soc. 113*, 8402−8409.

31. Burstein, E. A., Vedenkina, N. S., and Ivkova, M. N. (1973) *Photochem. Photobiol. 18*, 263−279.
32. Killenberg-Jabs, M., König, S., Eberhardt, I., Hohmann, S., and Hübner, G. (1997) *Biochemistry 36*, 1900−1905.
33. Farrenkopf, B., and Jordan, F. (1992) *Protein Expression Purif. 3*, 101−107.
34. Biaglow, J. E., Mieyal, J. J., Suchy, J., and Sable, H. Z. (1969) *J. Biol. Chem. 244*, 4054−4062.
35. Farzami, B., Mariam, Y. H., and Jordan, F. (1977) *Biochemistry 16*, 1105−1110.
36. Jordan, F., Akinyosoye, O., Dikdan, G., Kudzin, Z. H., and Kuo, D. J. (1988) in *Thiamin Pyrophosphate Biochemistry* (Schowen, R. L., and Schellenberger, A., Eds.) Vol. 1, pp 79−92, CRC Press, Boca Raton, FL.
37. Diefenbach, R. J., Candy, J. M., Mattick, J. S., and Duggleby, R. G. (1992) *FEBS Lett. 1*, 95−98.
38. Candy, M. J., Koga, J., Nixon, P. F., and Duggleby, R. G. (1996) *Biochem. J. 315*, 745−751.
39. Eftink, M. R., and Ghiron, C. A. (1976) *Biochemistry 15*, 672−680.
40. Eftink, M. R., and Ghiron, C. A. (1987) *Biochim. Biophys. Acta 916*, 343−349.
41. Divita, G., Müller, B., Immendörfer, U., Gautel, M., Rittinger, K., Restle, T., and Goody, R. S. (1993) *Biochemistry 32*, 7966−7971.
42. Kochetov, G. A., and Usmanov, R. A. (1970) *Biochem. Biophys. Res. Commun. 41*, 1134−1140.
43. Heinrich, C. P., Noack, K., and Wiss, O. (1971) *Biochem. Biophys. Res. Commun. 44*, 275−279.
44. Wikner, C., Meshalkina, L., Nilsson, U., Nikkola, M., Lindqvist, Y., and Schneider, G. (1994) *J. Biol. Chem. 269*, 32144−32150.
45. Ali, M. S., Shenoy, B. C., Eswaran, D., Andersson, L. A., Roche, T. E., and Patel, M. S. (1995) *J. Biol. Chem. 270*, 4570−4574.
46. Yi, J., Nemeria, N., McNally, A., and Jordan, F. (1996) *J. Biol. Chem. 271*, 33192−33200.
47. Hopmann, R. F. W. (1980) *Eur. J. Biochem. 110*, 311−318.
48. Ullrich, J. (1982) *Ann. N.Y. Acad. Sci. 378*, 287−305.
49. Kochetov, G. A., Usmanov, R. A., and Merzlov, V. P. (1970) *FEBS Lett. 9*, 265−266.

BI9902438